Available online at www.sciencedirect.com

ScienceDirect

Energy Procedia 97 (2016) 554 – 561

Energy Procedia

European Geosciences Union General Assembly 2016, EGU
Division Energy, Resources & Environment, ERE

San Pedro leucogranite from A Coruña, Northwest of Spain: Uses of a heritage stone

D.M. Freire-Lista[a]*, R. Fort[a], M.J. Varas-Muriel[a,b]

[a]*Instituto de Geociencias IGEO (CSIC, UCM) Spanish Research Council CSIC – Complutense University of Madrid UCM. Madrid 28040, Spain*
[c]*Facultad de CC. Geológicas. Complutense University of Madrid UCM. Madrid, 28040, Spain*

Abstract

San Pedro leucogranite from A Coruña, in the Northwest of Spain, has been a building stone widely used in the Middle Ages. Colour, rarity, appearance and petrophysical properties have led to the use of this leucogranite.
Monuments such as churches, tombstones and the basement of the Hercules Tower lighthouse, declared a UNESCO World Heritage Site in 2009, make it an ideal candidate for designation as a Global Heritage Stone Resource.

Peer-review under responsibility of the organizing committee of the General Assembly of the European Geosciences Union (EGU)

Keywords: leucogranite; building stone; petrophysic properties; decay

1. Introduction

Throughout history we can find many examples of locations that have been named based on the heritage stones encountered in the area. The heritage of a town is related to its geological environment, which provides building materials [1].

Not far from A Coruña city center (Spain) there is a mountain called Monte San Pedro, which has an etymological origin that is closely linked to stones that can be found in several historic quarries of different types of

* Corresponding author. Tel.: +34 913 944 903; fax: +34 915 425 353.
E-mail address: d.freire@igeo.ucm-csic.es

Peer-review under responsibility of the organizing committee of the General Assembly of the European Geosciences Union (EGU)
doi:10.1016/j.egypro.2016.10.075

granite. An area of this mountain is called *Penaboa* (good stone). In *Penaboa* there are several historic quarries of San Pedro leucogranite [2]. In the larger quarry, where extraction activity stopped in the second half of the twentieth century, a tourist elevator has been installed in order to enjoy the panoramic views from the top of the mountain. Very close to the base of the elevator, on the cliff, there is a small historical quarry of San Pedro leucogranite. Several mason marks have been found in this location, indicating that this quarry was used before the larger quarry. The peculiarity of the older quarry is that it is located next to the sea, which would facilitate the shipping of the stone. Diaclasses of the leucogranite have an optimal spacing for easy stone removal. This location is strategic for the dissemination of heritage stones [3] because of its proximity to the seaside promenade in A Coruña and to the new tourist infrastructures which have been built in the area.

San Pedro leucogranite appears locally in small isolated outcrops facing the NE-SW on the west side of the city of A Coruña, spreading from the villages of *Penaboa* to Pastoriza (figure 1). The orientation of the crystals that characterize the San Pedro leucogranite is due to the flow dynamic of the magma that rises to the surface during the Variscan orogeny deformation phase and this leucogranite comes into contact with a coarse-grained granodiorite. This granodiorite has gray tones and turns pink when it is altered. It has great mega crystals of twinned feldspars and quartz aggregates.

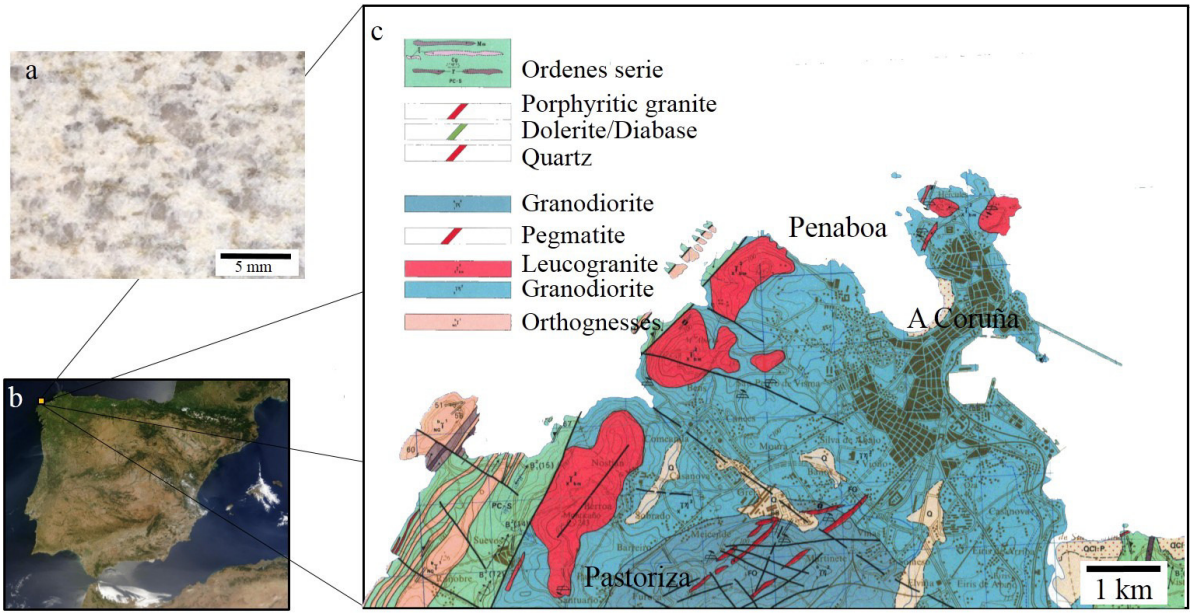

Fig. 1. (a) Hand sample of San Pedro leucogranite (b) Iberian Peninsula. Satellite view. Google maps; (c) Geological map of A Coruña area. IGME, 1975

Petrological characteristics such as appearance, colour, rarity, quality and durability of the San Pedro leucogranite are the main reasons for which this granite has been used for carving. These characteristics explain its wide use in the architectural history of the city of A Coruña and surrounding villages (figure 2). San Pedro leucogranite has also been used for ashlars, sculptures and architectural details.

Several scientific studies [2,4] have been conducted to understand the petrophysical properties of San Pedro leucogranite, both in fresh and altered states. The ultrasonic pulse velocity, mercury porosity, colour and hydric properties of the San Pedro leucogranite have been studied.

San Pedro leucogranite is proposed as a Global Heritage Stone Resource [5,6,7,8], showing its petrological characteristics used throughout history and decay. These characteristics and historical quarries should be given value due to its heritage significance.

Contact between leucogranite and granodiorite in the same historical ashlars are an indication of the *Penaboa* quarry origin. These ashlars reveal the scarcity of quality quarries of the San Pedro leucogranite in the Middle Ages, as masons used ashlars that reveal contact between the leucogranite and the granodiorite, forcing them to use these ashlars despite the fact that it lowered the quality of valuable sculptures full of detailed work such as the Romanesque columns of the main facade of the Santa María de Azogue Church and the Clara Sánchez tombstone (both in Betanzos) which are carved on ashlars where the contact between San Pedro leucogranite and granodiorite is remarkable (figure 2a).

2. Historical use of San Pedro leucogranite

In the Middle Age there was a boom in the use of the San Pedro leucogranite in Galician Romanesque sculptures. In the city centre of A Coruña, there are remarkable amounts of monuments such as the twelfth century Romanesque churches of Santa María del Campo [1] and Santiago. Subsequently, it has been used in Las Capuchinas Church [1], built in 1715 by the architect Fernando Casas y Novoa, which is now the location of the Fine Arts Museum. In 1766 and in 1794 both the monumental church of San Jorge [8] and the Neptune fountain were built using San Pedro leucogranite. In 1861 the basement of the Hercules Tower was finished using San Pedro leucograntie. This monument, with Roman origins is a majestic lighthouse in the city of A Coruña and was declared World Heritage by UNESCO in 2009. San Pedro leucogranite was used to pave the main tourist streets of the city of A Coruña (Calle Real and Cantones, to name the most popular) and has also been used in pavements, balconies, shields, stairs and spur stones [4,9] (Table 1 and figure 2). The most recent buildings built with San Pedro leucogranite were two groups of social housing: Pardo de Santallana and María Pita in the mid-twentieth century in the neighbourhood of Labañou, located very close to the historical quarries of San Pedro leucogranite.

Betanzos is a historical village about 25 km from A Coruña. Its historical centre was declared as a historic-artistic site in 1970. This village also has a great representation of San Pedro leucogranite in the sculptures and ashlars of the Santa María de Azogue church, where its portico, dating back to the late fourteenth century, was carved with San Pedro leucogranite. In addition, the San Francisco church, built in the fourteenth century, contained tombstones which were carved in San Pedro leucogranite. Two of the most important tombstones are the tombstones of Clara Sánchez, wife of the merchant Alfonso de Carvallido between 1450 and 1480, and Alonso Ianeiro, a judge in Betanzos during the fifteenth century. Both tombstones are now in the Archaeological Museum of Betanzos.

3. Methodology

Several blocks of San Pedro leucogranite were taken from the *Penaboa* quarry according to the split directions and the four cubic specimens measuring 50 ± 5 mm on each side that were cut from them. Specimen length was measured in the three orthogonal directions with a Mitutoyo digital calliper with a precision of ±0.01 mm. Four measurements were taken in each of the three directions and the average was calculated. Smaller fragments were also collected for thin section studies.

Colour was measured on a Minolta CM-700 D with a CM-S100WCOLOR DATA Software Spectra Magic NX spectrophotometer. Once each cubic sample had reached a constant mass, 10 colour measurements were taken on each face of the cubic specimens. The average of these measurements was calculated. The CIELAB system (CIELAB, 1976) colour parameters were used: luminosity (L*), red to green coordinate (a*), blue to yellow coordinate (b*) and yellow (YI*) and white (WI*) index. The measurement condition of the equipment was iluminate D65, with a diameter window measuring 6 mm in diameter.

In each of four cubic specimens, the ultrasound propagation velocity was measured in direct transmit/receive mode (transducers facing each other on opposite sides of the cubic specimen), and in the three spatial directions (XYZ).

Measurements were taken after the specimens were dried in an oven at 65º C to a constant weight (when the difference between two consecutive measurements, taken 24 h apart, was 1‰).

Table 1. Monuments built with San Pedro leucogranite

Heritage works	Year built
Santa María do Campo Church	12th century
Alonso Ianeyro tombstone	14th century
Santa María de Azogue Church	14th century
Scultures at San Francisco Church	1387
Capuchinas Church	1715
San Jorge Church	1766
Santa Bárbara convent	1786
Neptune fountain	1794
Pedestal of Hercules´ Tower	1861
Eusebio da Guardia memorial columns	20th century
Pardo de Santallana social house	1962

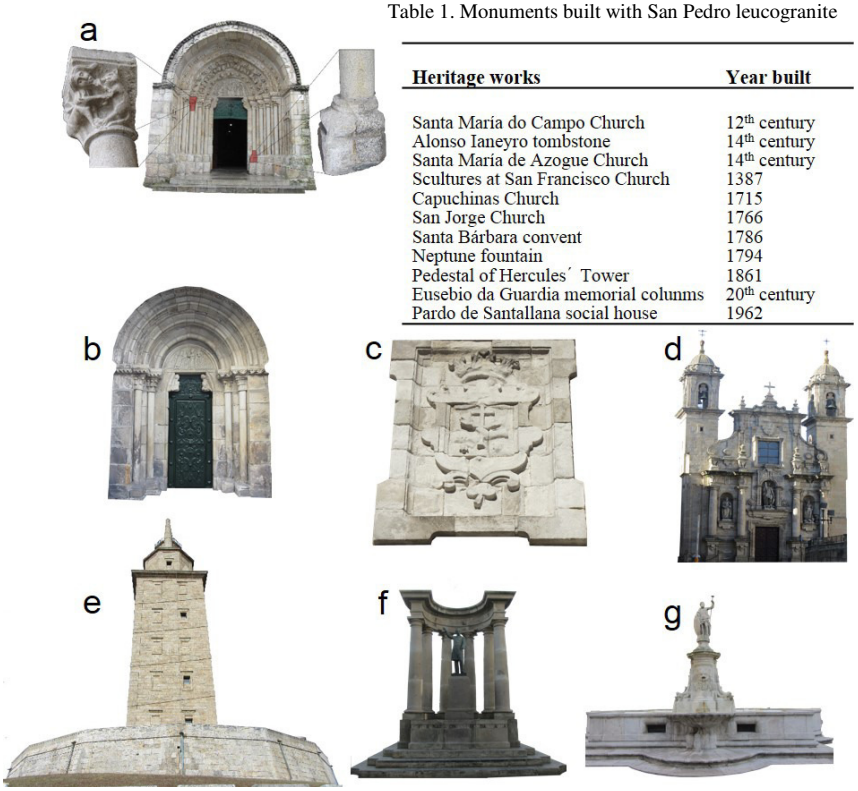

Fig. 2 (a) Base and capital of Santa María de Azogue church (14th century). Main facade. Betanzos, A Coruña; (b) Santa María do Campo church (12nd century), A Coruña; (c) Coat of arms. Capuchinas convent (18th century), A Coruña; (d) San Jorge church (18th century), A Coruña; (e) Hercules´ Tower pedestal (19th century), A Coruña; (f) Eusebio da Guardia memorial columns (20th century), A Coruña; (g) Neptune fountain, A Coruña; (18th century)

CNS Electronics PUNDIT test equipment, with a precision of ±0.1 μs, was used for the ultrasonic measurements. The system included transducers with a frequency of 1 MHz and a flat, round contact surface (11.82 mm in diameter). A water and carboxymethyl cellulose paste (Sichozell Kleister brand, by Henkel) was used to improve and increase the contact and bond between the stone surface and the transducer.

Material anisotropy can be determined by measuring the propagation velocity of ultrasound or P waves (Vp) in different directions in space [10]. In this study, the anisotropy indexes were found from the ultrasound propagation velocity measured in the materials under analysis. The indexes proposed by Guydader and Denis (1986).

$$dM\% = [1- (2Vp_{min} / (Vp_{mean} + V_{max}))] \times 100; \quad dm\% = [(2 \times (Vp_{max} - V_{mean}) / (Vp_{mean} + V_{max})] \times 100 \quad [11]$$

The three velocities shown in the anisotropy calculations refer to the velocities found for the three orthogonal directions in space: Vp_{max} is the mean maximum velocity obtained in any one of those directions, Vp_{min} is the mean minimum velocity and Vp_{mean} is the intermediate value.

Mercury intrusion porosimetry (MIP) was conducted on a single prismatic specimen (12 ± 2 mm in diameter and 20 ± 2 mm in height). The analysis was run after the sample was oven-dried to a constant weight at 70 °C. A Micromeritics' Autopore IV 9500 porosimeter with a maximum pressure of 414 MPa (60,000 psi) was used to assess sample pore structure, including total porosity (pore diameter range: 0.001–400 μm), macro- and micro-porosity and pore size distribution. The cut-off between micro- and macro-porosity was set at a pore diameter of 5 μm [12,13].

Two 30 × 20 ± 3 mm thin sections measuring, 30 μm thick were extracted from samples. Sawing was performed at low speed (120 rpm) and low strain so as not to generate artefacts (microcracks).

The thin sections were impregnated with fluorescence and characterised under an Olympus BX 51 polarized light microscope (PM) fitted with DP 12-coupled (6 V/2.5 Å) Olympus digital micrography and Olympus DP-Soft software (version 3.2). Microcracks were characterised with the same equipment, as well as with the same set-up using an Olympus U-RF-T mercury lamp fluorescence microscope (FM). PM and FM micrograph mosaics [14] were made from the thin sections to monitor microcracks. Each mosaic comprised 40 micrographs of the same area, measuring approximately 4.5 cm^2.

FM mosaic was laid over the same fragment of the PM mosaic and in this merger has made a network (1.5 × 2 cm) divided into squares measuring 5 × 5 mm (a total of 155 mm, linear) in each of the thin sections. The numbers of microcracks which intersect the sides of these networks have been measured to determine if the quartz, potassium feldspar, plagioclase or muscovite were affected. The number of microcracks was divided by the total length of the lines in the network to calculate the number of microcracks per linear millimetre (linear crack density — LCD) [15].

4. Results

The samples under study are light colored stones (95% leucocratic minerals) and have an inequigranular and faneritic texture. Their main mineralogical composition is made up of potassium feldspar, quartz and some muscovite. Minerals are slightly deformed and show a slight orientation. This leucogranite is fine-grained, with wide variation in sizes of the crystals, ranging from 2 mm to 60 μm.

The quartz appears as elongated anhedral crystals, providing the leucogranite with a marked orientated texture. The plagioclases are isolated or aggregate euhedral tabular crystals. The potassium feldspars are anhedral and interstitial. The muscovites are rare and in laminar form and appear isolated or aggregated.

San Pedro leucogranite is characteristically creamy white (a* and b* low) with high luminosity (L* ±83/100). The CIELAB scale (1976), L*,a*, b*, WI and YI indices are in the table 2a.

Table 2b reflect significant aspects of the San Pedro leucogranite porosity. Total Hg porosity is >4%. Of this porosity, almost 74% are micropores with less than 5 μm in diameter. It is concentrated mainly in the range between 1 and 5 μm (~56%) and between 0.1 and 1 μm (~23%). All of the minerals of the San Pedro leucogranite show more intracrystalline than intercrystalline microcracks. Table 2c below shows the number of intra- and intercrystalline in the main minerals. The lineal crack density is 2.3 in this leucogranite and potassium feldspar have the highest density of microcracks.

The microcracks propagation is through the leucogranite microstructure. That is to say, the microcracks follow the feldspar twins, the compositional zones and the outer limits of the crystals. The feldspars create a dense network of microcracks between the quartz, which have less intracrystalline microcracks.

The velocity of ultrasonic waves (Vp) are shown in table 2d below. Vp measured on the X axis is 4.8% higher than Vp measured on the Y axis and 42.9% higher than Vp measured on the Z axis. This indicates a high index of anisotropy with a dM index of 41%.

The distribution of the pores favors the circulation of fluids within the San Pedro leucogranite where exist high microporosity. This high microporosity favors chemical and physical decay process, especially gelifraction and salt crystallization [16,17,18].

Table 2. (a) Average colour coordinates; (b) Pore parameters of San Pedro leucogranite; (c) Number of inter- and intra-crystalline microcracks in 155 linear mm; (d) Ultrasonic pulse velocities. L*: lightness; a*: Red-green value; b*: Blue-yellow value; WI: Whiteness index; YI: Yellowness index; Vp: Ultrasonic wave velocity. dM: Total anisotropy. dm: Relative anisotropy; Qz: Quartz; K-Fsp: Potassium feldspar; Pl: Plagioclase; Ms: Muscovite.

a

Colour parameters	Value	Colour indices	Value
L*	82.8±2.2	YI	13.1±1.7
a*	1.3±0.2	WI	28.1±4.7
b*	7.4±1.0		

b

Pore parameters	Value
Real density (g/cm^3)	2.5
Bulk density (g/cm^3)	2.6
Total Hg porosity (%)	4.4
Microporosity (%)	73.9
Macroporosity (%)	26.1
Mean pore diameter (µm)	0.9
Tortuosity (µm)	11.1
Hg Permeability (mdarcy)	32.35

c

Mineral	Microcrack	Number
Qz	Inter-	38
	Intra-	46
K-Fsp	Inter-	65
	Intra-	78
Pl	Inter-	59
	Intra-	66
Ms	Inter-	3
	Intra-	4

d

Vp-Axes	Value	dM	dm
X	3011±136		
Y	2865±104	41	5
Z	1720±127		

5. San Pedro leucogranite decay

Microcracking is particularly important in the development of decay [19,20,21]. It is also important in increasing the porosity and permeability due to the number, type and connection of these microcracks per unit longitude as it facilitates the transmission of fluids [22,23]. The porosity and microcrack interconnection systems are conditioned by the degree of weathering [24].

Mineralogical orientation produces a strong anisotropy which is detected by ultrasound waves [25]. This high anisotropy can produce a negative effect on durability [10].

The circulation of liquids, salt or air pollutants accelerates decay. Generally, decay is concentrated at lower levels on ashlars on facades (4 meters above the ground). This is due to the size of the capilar pores [26,27]. The micropores facilitate the decay by salt crystallization, which produces salt efflorescences, alveolization [2], scaling [22], splintering, bursting, fragmentation [28], rounding and granular disaggregation due to the loss of quartz crystals, potassium feldspar fragmentation and plagioclase alteration [36]. Other types of decay are due to biological colonization by micro-organisms [4,29], black crust [29] and anthropic decay [30, 31].

The location of the historic quarries in the *Penaboa* cliff leads to weathering of the minerals, mainly chemical decay in feldspar and mechanical decay in quartz. This explains the 4% of Hg porosity and the existence of salt in the interior of the ashlars. That is to say, salt entered the leucogranite through microcracks previous [32,33] to their extraction from the quarries and being carved in workshops. Once the leucogranite has been put into use, decay can be caused by external agents such as climate and microclimate [34,35], orientation of the walls [22], concentration of loads [37], freezing and thawing [20], wetting and drying cycles and thermal shock [21]. In general, the less damaged facades are those that were built in much more modern ages due to the fact that ashlars are more recent and they have been extracted from deeper quarries where the quality of the leucogranite is better (having experienced a lesser degree of weathering than those found in the superficial quarries).

6. Conclusions

San Pedro leucogranite, quarried in the region of A Coruña, is present in the city's tangible and intangible heritage. It is characterised by high density, relative low porosity, high Vp and excellent durability.

The petrographic and petrophysical properties of San Pedro leucogranite, along with its durability and the historic quarries, make it eligible for designation as a Global Heritage Stone Resource. Its designation will contribute to

raised awareness of historic and modern features that are essential to its conservation and a will provide for more efficient use of the leucogranite as a restoration material in the heritage buildings.

Because the historical quarries were closed in the second half of the twentieth century, the enhancement by and knowledge of the authorities related to heritage building care for the future restoration of heritage buildings and also the location of these quarries, on the seafront of one of the major touristic cities in northern Spain, will give visibility to the importance of dimension stones used in heritage buildings.

Acknowledgements

This study was funded by the Community of Madrid under GEOMATERIALS 2 project S2013/MIT-2914 and conducted by members of the Complutense University of Madrid's Research Group: "Alteración y Conservación de los Materiales Pétreos del Patrimonio" (ref. 921349). The petrophysical assessments were run at the IGEO Petrophysical Laboratory, affiliated with the Moncloa Campus of International Excellence (UCM-UPM) Heritage Laboratory Network (RedLabPat).

References

[1] Fort R, Alvarez de Buergo M, Pérez-Monserrat EM, Gómez-Heras M, Varas-Muriel MJ, Freire-Lista, DM. Evolution in the use of natural building stone in Madrid, Spain. Quarterly Journal of Engineering Geology and Hydrogeology 2013; 46:421-429.

[2] Sanjurjo J, Alves CAS. Degradation of granitic rocks used as construction material in historic building of A Coruña (NW Spain). Cadernos Laboratorio Xeolóxico de Laxe 2006; 31:11-28.

[3] Micle D. Archaeological Heritage Between Natural Hazard and Anthropic Destruction: The Negative Impact of Social Non-involvement in the Protection of Archaeological Sites. Procedia - Social and Behavioral Sciences 2014; 163:269-278.

[4] Sanjurjo Sánchez J, Vidal Romaní JR, Alves C. Deposition of particles on gypsum-rich coatings of historic buildings in urban and rural environments. Construction and Building Materials 2011; 25:813-822.

[5] Cooper BJ. Toward establishing a "Global Heritage Stone Resource" designation. Episodes 2010; 33(1):38-41.

[6] Cooper BJ, Marker BR, Thomas IA. Towars International Designation of a Heritage Dimension Stone: Key Engineering Materials 2013; 548:329-335.

[7] Cooper BJ, Marker BR, Pereira D, Schouenborg B. Establishment of the "Heritage Stone Task Group" (HSTG): Episodes, 2013; 36(1):8-9.

[8] Freire-Lista DM, Fort R, Varas-Muriel MJ. Alpedrete granite (Spain). A nomination for the "Global Heritage Stone Resource" designation. Episodes 2015; 38 (2):106-113.

[9] Sanjurjo Sánchez J, Vidal Romaní JR, Alves C. Comparative analysis of coatings on granitic substrates from urban and natural settings (NW Spain) Geomorphology 2012; 138:231-242.

[10] Fort R, Varas MJ, Alvarez de Buergo M, Freire-Lista, DM. Determination of anisotropy to enhance the durability of natural stone: Journal of Geophysics and Engineering 2011; 8:132-144.

[11] Guydader J, Denis A. Propagation des ondes dans les roches anisotropes sous contrainte ´evaluation de la qualit´e des schistes ardoisiers Bulletin of Engineering Geology and the Environment 1986; 33:49-55.

[12] Russel, SA. Stone Preservation Committee Report (Appendix I). H.M. Stationary Office, London 1927.

[13] Rodríguez C, Sebastián E. Técnicas de análisis del sistema poroso de materiales pétreos ornamentales: usos y limitaciones. Ingeniería Civil, 1994; 96:130-142.

[14] Hooker JN, Larson TE, Eakin A, Laubach S, Eichhubl P, Fall A, Marrett R. Fracturing and fluid flow in a sub-décollement sandstone; or, a leak in the basement Journal of the Geological Society 2015; 172:428-442. doi:10.1144/jgs2014-128.

[15] Sousa LMO, Suarez del Rio LM, Calleja L, Ruiz de Argondona VG, Rey AR. Influence of microcracks and porosity on the physico-mechanical properties and weathering of ornamental granites. Engineering Geology 2005; 77:153-168.

[16] Liu Q, Huang S, Kang Y, Liu X. A prediction model for uniaxial compressive strength of deteriorated rocks due to freeze–thaw Cold Regions Science and Technology 2015; 120:96-107.

[17] Sajid M, Coggan J, Arif M, Andersen J, Rollinson G. Petrographic features as an effective indicator for the variation in strength of granites. Engineering Geology 2016; doi:10.1016/j.enggeo.2016.01.001.

[18] López-Arce P, Varas-Muriel MJ., Fernández-Revuelta B, Álvarez de Buergo M, Fort R, Pérez-Soba C. Artificial weathering of Spanish granites subjected to salt crystallization tests: surface roughness quantification. Catena 2010; 83, 170-185.

[19] Fort R, Alvarez de Buergo M, Pérez-Monserrat EM. Non-destructive testing for the assessment of granite decay in heritage structures compared to quarry stone. International Journal of Rock Mechanics & Mining Sciences 2013; 61:296-305.

[20] Freire-Lista DM, Fort R, and Varas-Muriel MJ. Freeze-thaw fracturing in building granites. Cold Regions Science and Technology 2015; 113:40-51.

[21] Freire-Lista DM, Fort R, and Varas-Muriel MJ. Thermal stress-induced microcracking in building granite. Engineering Geology 2016; 206:83-93.

[22] Freire-Lista DM, Fort R. Causes of scaling on brush hammered heritage ashlars. A case study: Plaza Mayor of Madrid (Spain). Environmental Earth Sciences 2016; DOI: 10.1007/s12665-016-5688-0.
[23] Hooker JN, Laubach SE, Marrett R. A universal power-law scaling exponent for fracture apertures in sandstone. Geological Society of America Bulletin 2014; 126: 9-10, p. 1340-1362. DOI: 10.1130/B30945.1.
[24] Siegesmund S, Török A. Building stones. In: Siegesmund S, Snethlage, R, editors. Stone in Architecture—Properties, Durability, fourth ed. Springer, Berlin; 2011. p. 11-96.
[25] Vázquez P, Alonso FJ, Esbert RM, Ordaz J. Ornamental granites: Relationships between p-waves velocity, water capillary absorption and the crack network. Construction and Building Materials 2010; 24(12):2536-2541.
[26] Moreno F, Vilela SAG, Antunes ASG, Alves CAS. Capillary-rising salt pollution and granitic stone erosive decay in the parish church of Torre de Moncorvo (NE Portugal)-implications for conservation strategy Journal of Cultural Heritage 2006; 7:56-66
[27] Mosquera MJ, Rivas T, Prieto B, Silva B. Capillary Rise in Granitic Rocks: Interpretation of Kinetics on the Basis of Pore Structure. Journal of Colloid and Interface Science 2000; 222 (1):41-45.
[28] Cuccuru S, Casini L, Oggiano G, Cherchi GP. Can weathering improve the toughness of a fractured rock? A case study using the San Giacomo granite. Bulletin of Engineering Geology and the Environment 2012; 71:557-567.
[29] Silva B, Aira N, Martínez-Cortizas A, Prieto B. Chemical composition and origin of black patinas on granite Science of The Total Environment 2009; 408(1):130-137.
[30] Pozo-Antonio JS, Rivas T, Fiorucci MP, López AJ, Ramil A. Effectiveness and harmfulness evaluation of graffiti cleaning by mechanical, chemical and laser procedures on granite. Microchemical Journal 2016. 125:1-9.
[31] Casal Porto M, Silva Hermo B, Delgado Rodrigues J. Agents and forms of weathering in granitic rocks used in monuments. Science, Technology and European Cultural Heritage 1991; 439-442.
[32] Sousa LMO, Oliveira AS, Alves IMC. Influence of fracture system on the exploitation of building stones: the case of the Mondim de Basto granite (north Portugal) Environmental Earth Sciences 2016. 75:39 doi 10.1007/s12665-015-4824-6.
[33] Takemura T, Golshani A, Oda M, Suzuki K. Preferred orientations of open microcracks in granite and their relation with anisotropic elasticity. International Journal of Rock Mechanics & Mining Sciences 2003. 40: 443-454.
[34] Freire-Lista DM, Gomez-Villalba LS, Fort R. Microcracking of granite feldspar during thermal artificial processes. Periodico di mineralogía 2015; 84 (3 A): 519-537.
[35] Momeni, A., Khanlari, G.R., Heidari, M., Bagheri, R., Bazvand, E., 2015. Assessment of physical weathering effects on granitic ancient monuments, Hamedan, Iran. Environ Earth Sci. 74:5181–5190. DOI 10.1007/s12665-015-4536-y.
[36] Vasconcelos G, Lourenço PB, Alves CAS, Pamplona J. Ultrasonic evaluation of the physical and mechanical properties of granites. Ultrasonics 2008; 48: 453-466.
[37] Sajid M, Arif M, 2014. Reliance of physico-mechanical properties on petrographic characteristics: consequences from the study of Utla granites, north-west Pakistan. Bulletin of Engineering Geology and Environment. doi 10.1007/s10064-014-0690-9.